THERMAL BUCKLING OF FUNCTIONALLY GRADED PLATES WITH CUTOUTS

S.C. Pradhan*

Abstract

Finite element formulation for the thermal buckling of moderately thick rectangular functionally graded material (FGM) plates is developed. This is based on the first order shear deformation theory (FSDT). One dimensional heat conduction equation is employed to represent the non-uniform temperature distribution across thickness of the FGM plate. Material properties of the plate are considered to be function of temperature. It is assumed that the material properties of the FGM plate vary as a power function along the plate thickness. Finite element code is developed and computation of critical thermal buckling temperature of the FGM plates is carried out. This computer program is validated with the results available in the literature. Further, finite element analysis is carried out to determine the thermal buckling of rectangular FGM plates with circular cutout. Uniform and non uniform temperature distributions across the plate thickness are considered. Further, effects of (i) plate aspect ratio, (ii) plate thickness to side ratio, (iii) power index 'k' (iv) size of the cutout and (v) the three different boundary conditions on the critical buckling temperature are studied.

***Keywords**: finite element analysis, thermal buckling, functionally graded material, temperature dependent, plate with cutout*

Nomenclature

a, b, h	= length, width and thickness of the rectangular plate
z	= thickness coordinate variable
d	= diameter of the plate cutout
k	= volume fraction index
V_c	= volume fraction of ceramic
V_m	= volume fraction of metal
E_f, E_m, E_c	= Young's moduli of FGM plate, metal and ceramic
v_f, v_m, v_c	= Poisson's ratios of FGM plate, metal and ceramic
α_f, α_m, α_c	= thermal expansion coefficients of FGM plate, metal and ceramic
K_f, K_m, K_c	= thermal conductivities of FGM plate, metal and ceramic
P_f	= FGM material property (E_f, v_f, K_f) dependent on temperature
P_c	= material property of ceramic
P_m	= material property of metal
P_{-1}, P_1, P_2, P_3	= temperature coefficients of constituent materials
T	= temperature
T_c, T_m	= specified temperature at ceramic and metal surfaces, respectively
ΔT	= temperature difference from a stress free state
u_0, v_0, w_0	= mid-plane displacements of plate
Φ_x, Φ_y	= midplane rotations
ε_x^0, ε_y^0, ε_{xy}^0	= midplane strains in respective planes
κ_x, κ_y, κ_{xy}	= midplane curvatures of plate in respective planes
π	= total potential energy of the plate
π_1	= strain energy of the plate
π_2	= word done by in plane loading of the plate
A_{ij}, B_{ij}, D_{ij}	= stiffness coefficients of composite material

* Assistant Professor, Department of Aerospace Engineering, Indian Institute of Technology Kharagpur, Kharagpur-721 302 West Bengal, India; Email : scp@aero.iitkgp.ernet.in

Manuscript received on 07 May 2007; Paper reviewed, revised and accepted on 17 Oct 2007

$\left[K_s^e\right]$ = element stiffness matrix

$\left[K_g^e\right]$ = element geometric matrix

$\left[\mathrm{F_i^e}\right]$ = element forcing function

$\left[K_0\right]$ = global stiffness matrix

$\left[K_g\right]$ = global geometric matrix

Introduction

Functionally Graded Materials (FGMs) are those in which the volume fractions of two or more materials are gradually varied as a function of position along certain dimension of the structure to obtain desired distribution of material properties. For example, the compositions are varied from a ceramic rich surface to a metal rich surface across thickness of a plate with a pre-defined volume fractions and power index of these two materials. The ceramic material provides the high temperature resistance due to its low thermal conductivity and the metal material prevents the fracture due to the thermal stresses and provides adequate stiffness to the FGM structure. The gradual change of material properties could be tailored as per the required applications. Thus, there is optimum usage of both constituent materials. The continuous change in the microstructure of functionally graded materials (FGMs) distinguishes them from the fibrereinforced laminated composite materials, which have a mismatch of mechanical properties across an interface of two discrete materials bonded together. As a result, the constituents of the fibre-matrix composites are prone to debonding at extremely high thermal loading. Additional problems include the presence of the residual stresses due to the difference in coefficients of thermal expansion of the fibre and matrix in the fibrereinforced-plastic (FRP) composites. FGMs are free from these problems. By gradually varying the volume fraction of the constituent materials in the FGMs, stronger and tougher materials are achieved. These properties make the functionally graded materials to be preferred for various aerospace, mechanical and medical applications. Further, applications of the FGMs have been widely observed in the high temperature environments, including thermal shock.

In view of the distinct advantages of functionally graded materials, a number of investigations dealing with thermal stresses and buckling have been reported in the literature.

Ravichandran [1] calculated thermal residual stresses, arising from the fabrication of a linearly elastic functionally graded material flat plate. Praveen and Reddy [2] investigated the response of functionally graded ceramic-metal plates using finite element method. They have taken into account transverse shear strains, rotary inertia and moderately large rotations. Pradhan et.al [3] carried out the vibration characteristics of the FGM cylindrical shells. Cho and Oden [4] carried out finite element analysis of the effect of material variation through the thickness and the size of the FGM layer on thermomechanical characteristics for plane stress two-dimensional Ni-Al_2O_3 FGMs under uniform heating. Reddy [5] developed theoretical formulation and finite element model. He studied thermo-mechanical coupling, time dependency and geometric non-linearity behavior. Woo and Maguid [6] studied the nonlinear behaviour of the FGM plates and shallow shells. Green's function is employed by Kim and Noda [7] to analyze the deflection and transient temperature distribution of a FGM plate. Tsukamoto [8] formulated inelastic constitutive relations micro mechanically and the thermal stresses in FGM plates are obtained using micro mechanical approach. Yang et. al [9] analyzed the large amplitude, linear and nonlinear vibration behavior of pre-stressed laminated plates by thermo-electro-mechanical loading. Ma and Wang [10] studied the axisymmetric large deflection bending of a functionally graded circular plate under mechanical, thermal and combined thermal mechanical loadings. They employed classical nonlinear von Karman plate theory for the analysis. Croce and Venini [11] presented a family of finite elements for the Reissner-Mindlin functionally graded plates based on variational formulation. Najafizadeh and Heydari [12] analyzed the thermal buckling of FGM circular plate using third order plate theory. Lanhe [13] employed the first order shear deformation theory for obtaining equilibrium and stability equations for FGM plate. He carried out buckling analysis for different types of thermal loadings.

Pradhan [14] investigated the vibration suppression of FGM shells embedded with magnetostrictive layers. Shen [15] carried out post buckling analysis for a simply supported, shear deformable FGM plate with piezoelectric actuators. His work included combined action of mechanical, electrical and thermal loads. He assumed material properties to be temperature dependent. Sladeka et. al [16] employed a meshless local Petro-Galerkin approach and carried out stress analysis in two dimensional, anisotropic and linear elastic-plastic FGM.

Yang et. al [17] presented the effect of the inherent randomness of the FGM's on the elastic buckling of rectangular FGM plates resting on elastic foundation. Dai et. al [18] employed element-free Galerkin method to derive the shape functions using the moving least square method for analyzing the functionally graded material plates with distributed piezoelectric sensors and actuators. Kyung and Kim [19] investigated three dimensional thermo-mechanical buckling analysis for FGM plate by using three dimensional finite element method. They assumed material properties are temperature dependent and employed time discretization Crank-Nicholson method. Huang and Shen [20] analyzed the nonlinear vibration and dynamic response of a functionally graded material plate with surface bonded piezoelectric layers in thermal environments. They employed higher order shear deformation plate theory.

Study of thermal buckling of composite materials are important. Chang and Shiao [21] carried out thermal buckling analysis of isotropic and composite plates with cutouts. Chen [22] reported the thermal buckling results of thick composite laminated plates under non-uniform temperature distribution. Prabhu and Dhanraj [23] reported the thermal buckling of composite plates.

However, research reports in the area of thermal buckling of FGM plates with cutouts are limited. In the present work, computation is carried out for thermal buckling of FGM plates with cutouts. Material properties are assumed to be function of temperature. Effects of plate aspect ratio, plate thickness to side ratio, power index 'k, size of the cutout and three different types of boundary conditions on the critical buckling temperature are studied.

Mathematical Formulation

Consider a rectangular plate made of a mixture of metal and ceramic as shown in Fig.1. The material properties are gradually varied from bottom surface metal to top surface ceramic. An exploded view with granules of section A-A of Fig.1 is shown in Fig.2. This depicts the gradation from pure metal to pure ceramic across the thickness. Effective material properties P_f, like Young's modulus 'E' and thermal expansion coefficient 'α' are expressed as in original contribution Pradhan(14).

$$P_f = P_c V_c + P_m V_m \tag{1}$$

where, V_s denotes the volume fraction of the ceramic. This is expressed as

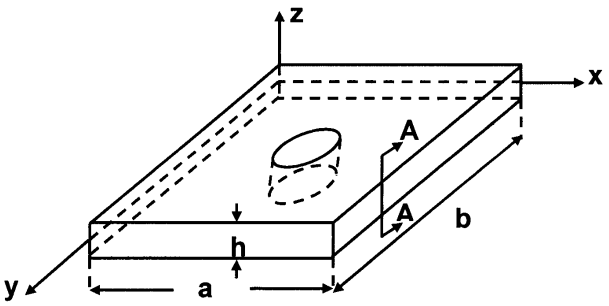

Fig.1 Schematic of rectangular FGM plate

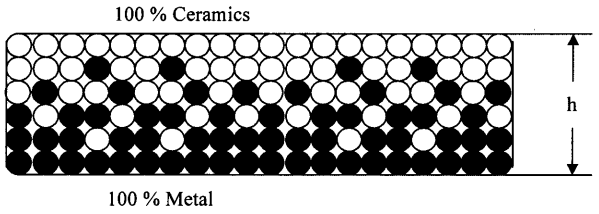

Fig.2 Section A-A (Fig.1) showing the gradation of metal and ceramic across the plate thickness

$$V_c = \left(\frac{2z+h}{2h}\right)^k \text{ where, } -h/2 \le z \le h/2 \tag{2}$$

$$V_c + V_m = 1 \tag{3}$$

k is the volume fraction index. From Eq. (1) and Eq. (2) the modulus of elasticity 'E', the coefficient of thermal expansion '*a*', and the thermal conductivity 'K' are expressed as,

$$\begin{aligned} E_f &= (E_c - E_m)\, V_c + E_m \\ \alpha_f &= (\alpha_c - \alpha_m)\, V_c + a_m \\ K_f &= (K_c - K_m)\, V_c + K_m \end{aligned} \tag{4}$$

Poisson's ratio '*v*' is assumed to be 0.3 for both the materials. In actual case, material properties are dependent on the temperature. Change in temperature does affect the strength and stiffness of the FGM plate. Thus it is necessary to include the effects of temperature in the thermal buckling analysis of the FGM plate. Material properties as a function of temperature are employed in the analysis. Material properties can be expressed as a nonlinear function of temperature

$$P_f = P_0 (P_{-1} T^{-1} + 1 + P_1 T^1 + P_2 T^2 + P_3 T^3) \tag{5}$$

Poisson's ratio '*v*' depends weakly on temperature change and is assumed to be constant. The temperature change across the thickness of the FGM plate is governed by one dimensional Fourier heat conduction equation as mentioned by Wu Lanhe [13]

$$\frac{d}{dz}\left[K(z)\frac{dT}{dz}\right] = 0 \qquad T = T_c \quad at \quad z = h/2$$
$$T = T_m \quad at \quad z = -h/2 \qquad (6)$$

where, T_c, T_m are specified temperature at ceramic and metal surfaces, respectively. Substituting conductivity expression in the Eq. (6) and solving the equation following expressions are obtained, Shen and Noda [24].

$$T(z) = T_m + \frac{\Delta T}{C}\left[\left(\frac{2z+h}{2h}\right) - \frac{K_{cm}}{(k+1)K_{cm}}\left(\frac{2z+h}{2h}\right)^{k+1} + \frac{K_{cm}^2}{(2k+1)K_{cm}^2}\left(\frac{2z+h}{2h}\right)^{2k+1} + h.o.t\right]$$

with

$$C = 1 - \frac{K_{cm}}{(k+1)K_{cm}} + \frac{K_{cm}^2}{(2k+1)K_{cm}^2} - \frac{K_{cm}^3}{(3k+1)K_{cm}^3} + h.o.t. \qquad (7)$$

$$\Delta T = (T_c - T_m)$$
$$K_{cm} = K_c - K_m$$

In the present analysis FSDT is employed. This accounts for transverse shear strains, which are represented as constant through the plate thickness. This theory requires shear correction coefficients to compute transverse shear force. The FGM plate of total thickness '*h*' is considered. The xy-plane is taken to be the midplane of the plate with the z-axis positive upward. Further, present formulation is restricted to linear elastic material behavior, small strains and displacements. To account for transverse shear deformation in the plate, the displacement components are expressed as

$$U(x,y,z) = u_0(x,y) + z\,\Phi_x(x,y)$$
$$V(x,y,z) = v_0(x,y) + z\,\Phi_y(x,y)$$
$$W(x,y,z) = w_0(x,y) \qquad (8)$$

The strain-displacement equations of linear elasticity case are written as,

$$\varepsilon_x = \frac{\partial u_0}{\partial x} + z\frac{\partial \Phi_x}{\partial x} = \varepsilon_x^0 + z\,\kappa_x$$
$$\varepsilon_y = \varepsilon_y^0 + z\,\kappa_y$$
$$\varepsilon_{xy} = \varepsilon_{xy}^0 + z\,\kappa_{xy}$$
$$\varepsilon_{xz} = \frac{\partial w_0}{\partial x} + \Phi_x$$
$$\varepsilon_{yz} = \frac{\partial w_0}{\partial y} + \Phi_y \qquad (9)$$

The constitutive relations are written as

$$\begin{Bmatrix}\sigma_x\\ \sigma_y\\ \sigma_{xy}\\ \sigma_{xz}\\ \sigma_{yz}\end{Bmatrix} = \begin{bmatrix}Q_{11} & Q_{12} & 0 & 0 & 0\\ Q_{12} & Q_{22} & 0 & 0 & 0\\ 0 & 0 & Q_{66} & 0 & 0\\ 0 & 0 & 0 & Q_{54} & 0\\ 0 & 0 & 0 & 0 & Q_{44}\end{bmatrix}\begin{Bmatrix}\varepsilon_x - \alpha\Delta T\\ \varepsilon_y - \alpha\Delta T\\ \varepsilon_{xy}\\ \varepsilon_{xz}\\ \varepsilon_{yz}\end{Bmatrix} \qquad (10)$$

where,

$$Q_{11} = Q_{22} = \frac{E_f}{1-v^2};$$

$$Q_{12} = v\,Q_{11};\; Q_{44} = Q_{55} = Q_{66} = \frac{E_f}{2(1+v)}$$

The stress resultants are expressed as

$$\begin{Bmatrix}N_x\\ N_y\\ N_{xy}\end{Bmatrix} = \int_{-h/2}^{h/2}\begin{Bmatrix}\sigma_x\\ \sigma_y\\ \sigma_{xy}\end{Bmatrix} dz$$

and

$$\begin{Bmatrix}Q_x\\ Q_y\end{Bmatrix} = \int_{-h/2}^{h/2}\begin{Bmatrix}\sigma_{xz}\\ \sigma_{yz}\end{Bmatrix} dz \qquad (11)$$

The moment resultants are written as

$$\begin{Bmatrix} M_x \\ M_y \\ M_{xy} \end{Bmatrix} = \int_{-h/2}^{h/2} \begin{Bmatrix} \sigma_x \\ \sigma_y \\ \sigma_{xy} \end{Bmatrix} z\, dz \qquad (12)$$

Substituting Eqns. (8-10) in Eqns. (11-12)

$$\begin{Bmatrix} N_x \\ N_y \\ N_{xy} \\ M_x \\ M_y \\ M_{xy} \end{Bmatrix} = \begin{bmatrix} A_{ij} & B_{ij} \\ B_{ij} & D_{ij} \end{bmatrix} \begin{Bmatrix} \varepsilon_x^0 \\ \varepsilon_y^0 \\ \varepsilon_{xy}^0 \\ \kappa_x \\ \kappa_y \\ \kappa_{xy} \end{Bmatrix} - \begin{Bmatrix} N_{tx} \\ N_{ty} \\ 0 \\ M_{tx} \\ M_{ty} \\ 0 \end{Bmatrix}$$

where i, j = 1, 2, 6 (13)

$$\begin{Bmatrix} Q_x \\ Q_y \end{Bmatrix} = \begin{bmatrix} A_{55} & 0 \\ 0 & D_{44} \end{bmatrix} \begin{Bmatrix} \varepsilon_{xz} \\ \varepsilon_{yz} \end{Bmatrix} \qquad (14)$$

where, $A_{ij}, B_{ij}, D_{ij} = \int_{-h/2}^{h/2} Q_{ij}\,(1, z, z^2)\, dz$ for i, j = 1,2,6

$$A_{ij} = \int_{-h/2}^{h/2} k_s\, Q_{ij}\, dz \qquad \text{for i, j = 4, 5}$$

where, k_s, = 5/6 is considered to account for the effect of transverse strains.

Thermal force and moments are given as,

$$\left[N_t\right] = \int_{-h/2}^{h/2} Q_{ij} \begin{Bmatrix} \alpha\Delta T \\ \alpha\Delta T \\ 0 \end{Bmatrix} dz$$

and

$$\left[M_t\right] = \int_{-h/2}^{h/2} Q_{ij} \begin{Bmatrix} \alpha\Delta T \\ \alpha\Delta T \\ 0 \end{Bmatrix} z\, dz \qquad (15)$$

where, ΔT is the applied temperature.

Field variables used are u, v, w, Φ_x, Φ_y which denote in plane, normal displacements and rotations, respectively. Eight noded isoparametric element is employed for the analysis. The generalized displacements are approximated over an element by

$$\{q\} = \sum_{i=1}^{8} \left[N_i\right] \left\{q_i^e\right\} \qquad (16)$$

where, $\left\{q_i^e\right\} = \left[u_{0i}\ v_{0i}\ w_{0i}\ \Phi_{x\,i}\ \Phi_{yi}\right]^T$. N_i is the shape function.

Midplane strains and curvatures are written in terms of generalized degree of freedom

$$\{\varepsilon\} = \{\varepsilon^0\} + z\{\kappa\} \qquad (17)$$

where, $\{\varepsilon\} = \left\{\varepsilon_x \quad \varepsilon_y \quad \varepsilon_{xy}\right\}^T$

$$\{\varepsilon^0\} = \sum_{i=1}^{8} \left[B_{ti}\right] \left\{q_i^e\right\}, \quad \{\kappa\} = \sum_{i=1}^{8} \left[B_{bi}\right] \left\{q_i^e\right\},$$

$$\begin{Bmatrix} \varepsilon_{xz} \\ \varepsilon_{yz} \end{Bmatrix} = \sum_{i=1}^{8} \left[B_{si}\right] \left\{q_i^e\right\} \qquad (18)$$

where

$$\left[B_{ti}\right] \begin{bmatrix} \dfrac{\partial N_i}{\partial x} & 0 & 0 & 0 & 0 \\ 0 & \dfrac{\partial N_i}{\partial x} & 0 & 0 & 0 \\ \dfrac{\partial N_i}{\partial y} & \dfrac{\partial N_i}{\partial x} & 0 & 0 & 0 \end{bmatrix}$$

$$\left[B_{b\,i}\right]\begin{bmatrix} 0 & 0 & 0 & \dfrac{\partial N_i}{\partial x} & 0 \\ 0 & 0 & 0 & 0 & \dfrac{\partial N_i}{\partial y} \\ 0 & 0 & 0 & \dfrac{\partial N_i}{\partial y} & \dfrac{\partial N_i}{\partial x} \end{bmatrix}$$

$$\left[B_{s\,i}\right] = \begin{bmatrix} 0 & 0 & \dfrac{\partial N_i}{\partial x} & N_i & 0 \\ 0 & 0 & \dfrac{\partial N_i}{\partial y} & 0 & N_i \end{bmatrix} \tag{19}$$

$[B_b]$, $[B_t]$ and $[B_s]$ corresponds to bending, tensile and shear strain-displacement matrices, respectively. Total potential energy is the sum of the strain energy and the work done by the in-plane loading.

$$\pi = \pi_1 + \pi_2 \tag{20}$$

where π_1 is the strain energy and π_2 is work done by the in-plane loading due to temperature change. Strain energy is expressed as

$$\pi_1 = \frac{1}{2}\int\int\int_v \{\varepsilon\}\{\sigma\}\,dV \tag{21}$$

Converting the volume integral into surface integral,

$$\pi_1 = \frac{1}{2}\int\int_R \left[N_x\varepsilon_x + N_y\varepsilon_y + N_{xy}\varepsilon_{xy} + Q_x\varepsilon_{xz} + Q_y\varepsilon_{yz}\right] dx\,dy \tag{22}$$

work done by inplane thermal loading is written as

$$\pi_2 = \frac{1}{2}\int_\Omega \left[N_x\left(\frac{\partial w}{\partial x}\right)^2 + N_y\left(\frac{\partial w}{\partial y}\right)^2 + 2N_{xy}\left(\frac{\partial w}{\partial x}\right)\left(\frac{\partial w}{\partial y}\right)\right] dA \tag{23}$$

Substituting Eqs. (13-17) in terms of strain matrices in Eqs.(22-23)

$$\pi_1 = \sum_{e=1}^{n}\left\{\frac{1}{2}\{q^e\}^T\left[K_s^e\right]\{q^e\} - \{q^e\}^T\left[R_t^e\right]\right\}$$

$$= \frac{1}{2}\{q\}^T\left[K_s\right]\{q\} - \{q\}^T\left[F_t\right] \tag{24}$$

$$\pi_2 = \sum_{e=1}^{n}\frac{1}{2}\{q^e\}^T\left[K_g^e\right]\{q^e\}$$

$$\pi_2 = \frac{1}{2}\{q\}^T\left[K_g\right]\{q\} \tag{25}$$

Elemental stiffness matrix is expressed as

$$\left[K_s^e\right] = \int\int_e \left\{\left[\chi_1\right]+\left[\chi_2\right]+\left[\chi_3\right]+\left[\chi_4\right]+\left[\chi_5\right]\right\} dx\,dy \tag{26}$$

where,

$$\left[\chi_1\right] = \left[B_t\right]^T\left[A\right]\left[B_t\right],\ \left[\chi_2\right] = \left[B_t\right]^T\left[B\right]\left[B_b\right],$$

$$\left[\chi_3\right] = \left[B_b\right]^T\left[B\right]\left[B_t\right],\ \left[\chi_4\right] = \left[B_b\right]^T\left[D\right]\left[B_b\right],$$

$$\left[\chi_5\right] = \left[B_s\right]^T\left[\bar{A}\right]\left[B_s\right] \tag{27}$$

$[B_b]$, $[B_t]$ and $[B_s]$ corresponds to bending, tensile and shear strain-displacement matrices, respectively. $[\bar{A}]$ is written as

$$\left[\bar{A}\right] = \begin{bmatrix} A_{55} & 0 \\ 0 & A_{44} \end{bmatrix} \tag{28}$$

Element geometric stiffness matrix is expressed as

$$\left[K_g^e\right] = \iint_e \left[B_g\right]^T\left[N_0\right]\left[B_g\right] dx\,dy \tag{29}$$

where,

$$N_0 = \begin{bmatrix} N_x & N_{xy} \\ N_{xy} & N_y \end{bmatrix} \text{ and}$$

$$\left[B_{g\,i}\right] = \begin{bmatrix} 0 & 0 & \dfrac{\partial N_i}{\partial x} & 0 & 0 \\ 0 & 0 & \dfrac{\partial N_i}{\partial y} & 0 & 0 \end{bmatrix} \tag{30}$$

Element thermal load vector is written as,

$$\left\{F_t^e\right\} = \iint_e \left\{ \left[B_t\right]^T \left\{N_t\right\} + \left[B_b\right]^T \left\{M_t\right\} \right\} d\,x\,d\,y \tag{31}$$

For pre-buckling displacements, first variation of strain energy is equated to zero,

$$\delta\pi_1 = 0$$

This yields

$$\left[K_0\right]\left\{q\right\} = \left\{F_t\right\} \tag{32}$$

For the critical buckling state corresponding to the neutral equilibrium condition, second variation of total potential energy is equated to zero. Finally, one obtains

$$\left| [K_0] + \lambda\,[K_g] \right| = 0 \tag{33}$$

where λ is determined by solving the above eigenvalue problem. The product of λ and the temperature difference ΔTcorresponds to critical buckling temperature T_{cr} of the FGM plate.

Validation

Developed finite element computer code is first validated for an isotropic plate as mentioned in Boley and Weiner [25] and Chen [22]. As a particular case of FGM material, when the volume fraction index *k* is considered to be 0, the FGM material behaves exactly as isotropic and homogeneous material. Material properties of Chen [22]. E_1/E_2 = 1, a/h = 100, ν = 0.3, α = 1x10^{-6}/^{0} C are employed. A refined finite element mesh of two thousand eight node quadrilateral elements is employed for the analysis. Critical buckling temperatures are computed.

Table-1 shows the comparison of non-dimensional critical buckling temperature of isotropic plate subjected to uniform temperature distribution with those of Boley and Weiner [25] and Chen [22]. From Table-1, it is observed that the present computed critical temperatures agree with those reported in the literature Boley and Weiner [25] and Chen [22].

Table-1 : Non-dimensional critical buckling temperature $T_{cr} = \lambda\Delta T \times \alpha \times 10^4$ for isentropic plate

a/b ratio	Boley and Weiner [25] (T_{cr})	Chen [22] (T_{cr})	Present analysis (T_{cr})
0.25	0.686	0.691	0.691
0.5	0.808	0.814	0.808
1.0	1.283	1.319	1.315
1.5	2.073	2.101	2.085
2.0	3.179	3.191	3.205
2.5	4.599	4.601	4.612
3.0	6.332	6.330	6.333

A FGM plate problem from reference Lanhe [13] is also considered for validating the present analysis. Material used for validation is alumina and aluminum as the ceramic and the metal, respectively. Material properties employed in the computation are listed in Table-2.

Thermal buckling temperature of FGM plates under uniform temperature are computed. Uniform temperature of 300°C is applied to the FGM plate. Predicted critical buckling temperatures for simply supported FGM plate *vs.* thickness to side ratio are plotted in Fig.3. In Fig.3, results obtained from the present analysis and results reported by Lanhe [13] are compared. From this figure one could note that the difference between the results obtained from present analysis and those reported in reference Lanhe [13] is less than two percent. Further, thermal buckling of simply supported FGM plate under nonuniform temperatures are computed. Critical buckling temperature *vs.* volume fraction index '*k*' of the FGM plate are plotted in

Table-2 : Material properties of alumina and aluminium, Pradhan [14]

Material properties	Alumina	Aluminium
E	380 GPa	70 GPa
K	10.4 $\frac{W}{mk}$	104 $\frac{W}{mk}$
α	7.4 x 10^{-6}/^0C	23 x 10^{-6}/^0C
ν	0.3	0.3

Fig.4. Results reported by Lanhe [13] are also plotted in this figure. In this figure one could notice that the present results and those reported in reference Lanhe [13] are in good agreement.

Results and Discussion

To study the thermal buckling of a rectangular FGM plate with circular cutout is carried out. Finite element analysis is employed. Only square plate results are presented. A typical one quarter finite element mesh of the quarter square plate consists of 1033 nodes and 320 quadratic eight node elements is depicted in Fig.5. However, a refined full size finite element mesh of four thousand such elements is employed for the analysis. The FGM plate is considered to be made of silicon nitride and stainless steel. Mechanical properties of these materials are listed in Table-3. In the analysis material properties of the constituent materials are considering to be function of temperature as mentioned in Eq. (5). Temperature dependent constants of silicon nitride and stainless steel are listed in Table-4.

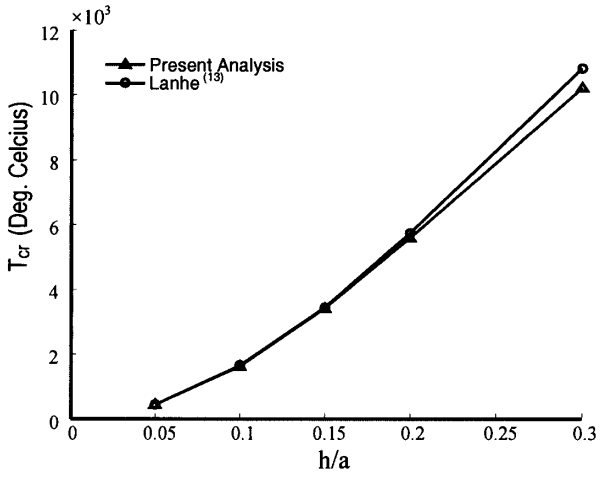

Fig.3 Critical buckling temperature of simply-supported FGM plate (a/b=1, k=0)

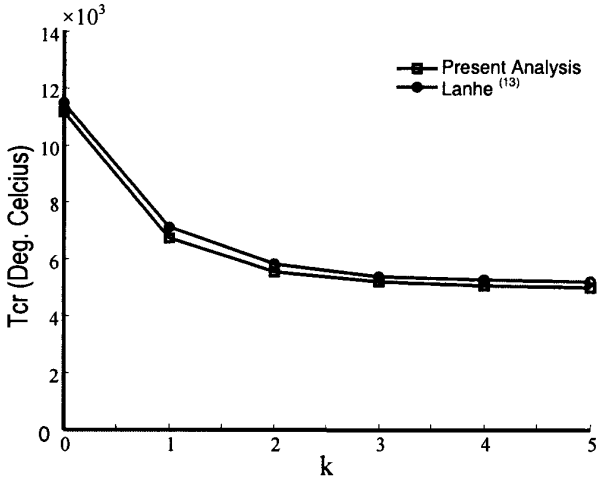

Fig.4 Critical buckling temperature of simply-supported FGM plate (a/b=1, h/a=0.2)

Following three different boundary conditions are considered for the computation of the Material Properties critical buckling temperatures of the FGM plate with cutout. BC1, all the sides are simply supported (SSSS), BC2, all the sides are clamped (CCCC) and BC3 two opposite sides are clamped and other two sides are simply supported (CCSS). Thus following degrees of freedoms are restrained for the three boundary conditions:

$$\text{BC1 : at } x = 0, a;\ u = w = \Phi_y = 0$$
$$\text{at } y = 0, b;\ v = w = \Phi_y = 0 \qquad (35)$$

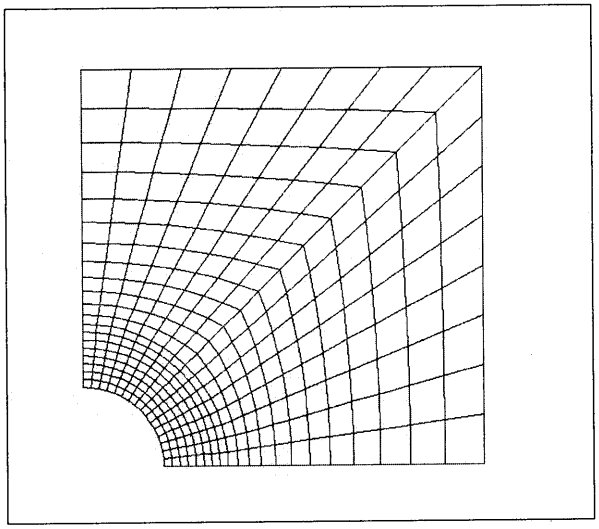

Fig.5 Finite element mesh of FGM square plate with circular cutout

Table-3 : Material properties of Silicon Nitride and Stainless Steel, Shen and Noda [24]

Material Properties	Silicon Nitride	Stainless Steel
E (GPa)	348.43	201.04
$K\left(\frac{W}{mk}\right)$	13.72	15.38
α (x $10^{-6}/^0 C$)	5.87	12.33
ν	0.3	0.3

Table-4 : Material constants of Silicon Nitride and Stainless Steel, Shen and Noda [24]						
Material	Properties	P_0	P_{-1}	P_1	P_2	P_3
Silicon Nitride	E_c	348.43e+9	0	-3.07e-4	2.16e-7	-8.946e-11
	α_c	5.8723e-6	0	9.095e-4	0	0
	K_c	13.723	0	0	0	0
Stainless Steel	E_m	201.04e+9	0	3.079e-4	-6.534e-7	0
	α_m	12.33e-6	0	8.086e-4	0	0
	K_m	15.379	0	0	0	0

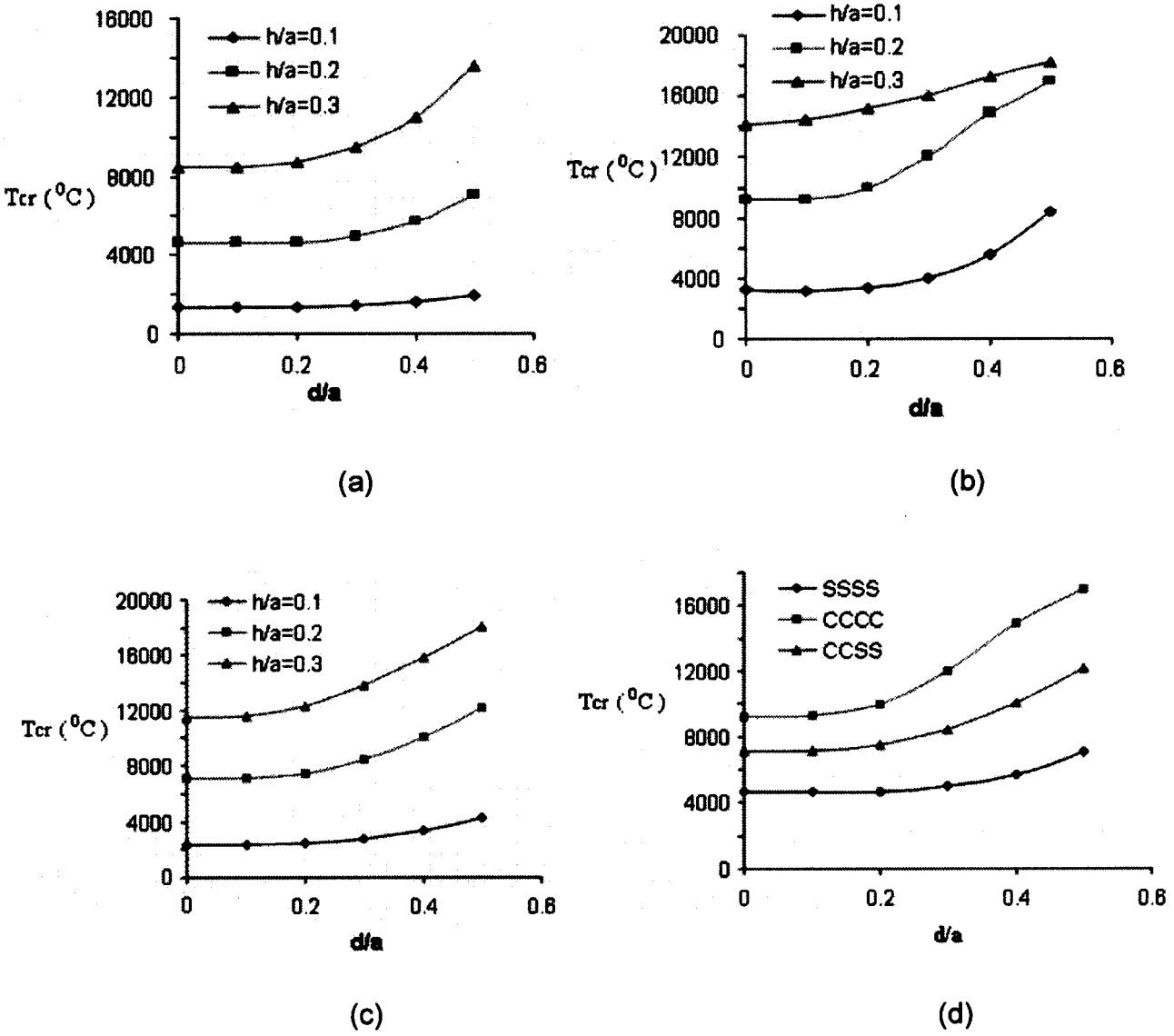

Fig.6 Critical buckling temperature vs the sizes of the cutout in the FGM plate under uniform temperature, (a/b=1, k=1) for (a) BC1 (b) BC2, (c) BC3 boundary conditions and (d) BC1, BC2 and BC3 boundary conditions (h/a=0.2)

BC2 : at x = 0, a; $u = v = w = \Phi_x = \Phi_y = 0$

at y = 0, b; $u = v = w = \Phi_x = \Phi_y = 0$ (36)

and

BC3 : at x = 0, a; $u = v = w = \Phi_x = \Phi_y = 0$

at y = 0, b; $v = w = \Phi_x = 0$ (37)

Critical thermal buckling load of the rectangular FGM plate with circular cutouts has been computed for various cases. The FGM plate subjected to uniform and non-uniform temperature loading are considered. Fig.6 shows the critical buckling temperatures of FGM plate under uniform temperature distribution for various thickness to side (h/a) ratios and different boundary conditions. In this figure one can note that buckling temperature increases gradually with increase in cutout size in case of all edges simply supported case BC1 and clamped-simply supported BC3 case. But in case of all edge clamped BC2, critical buckling temperature increases rapidly as cutout size increases. Buckling temperature also increases with increase of h/a ratio. It also shows that buckling temperature is highest for all sides clamped BC2 case. Fig.7 shows the effect of volume fraction index variation on critical buckling temperature. It shows that, buckling temperature decreases with increase in volume fraction. There is rapid decrease in buckling temperature as power index *k* in-

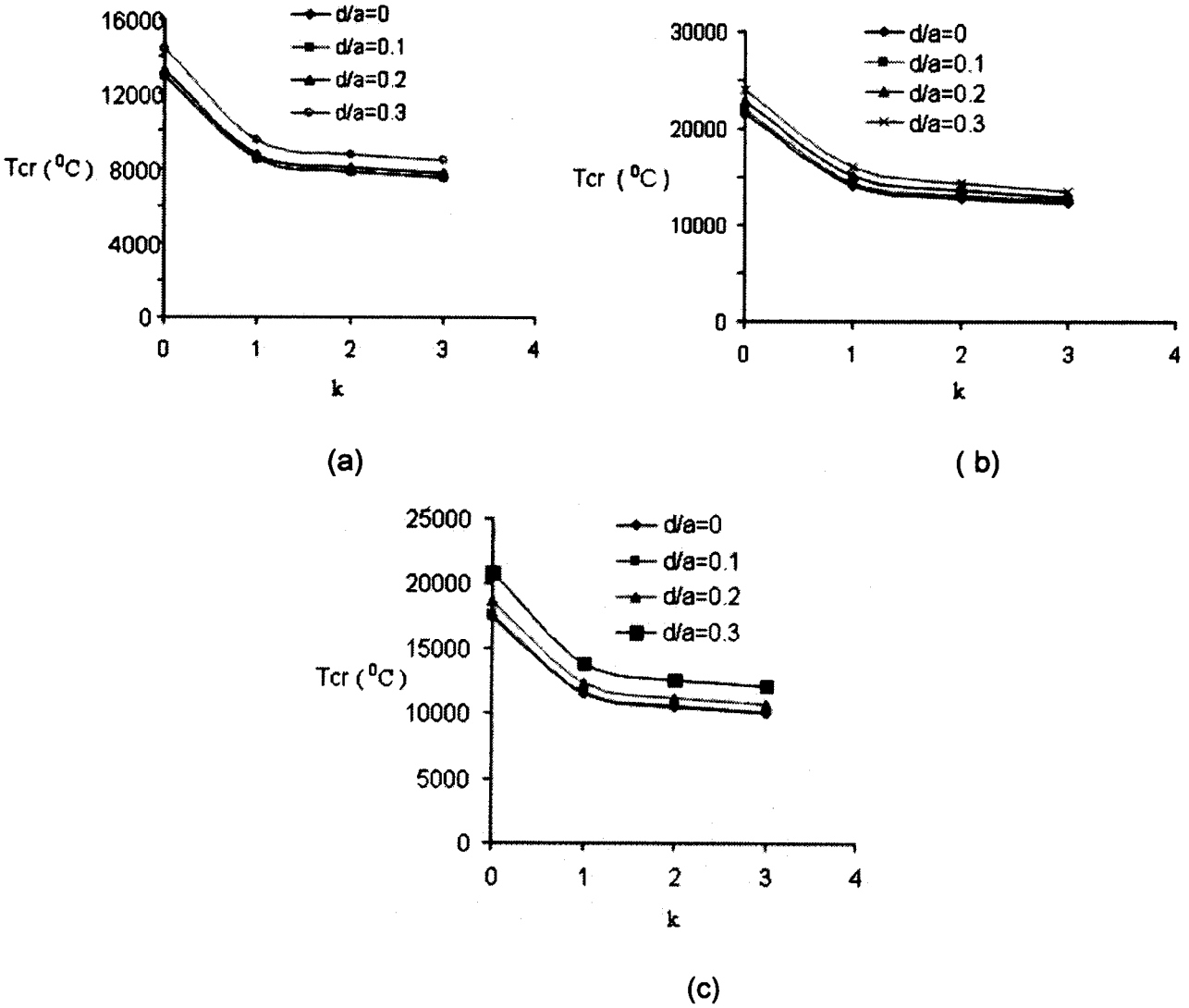

Fig.7 Critical buckling temperature vs power index 'k' of the FGM plate under uniform temperature, (a/b=1, h/a=0.3) (a) BC1 (b) BC2 and (c) BC3 boundary conditions

crease from 0 to 2. When *k* is greater than 2 buckling temperature almost remains constant for BC1 and BC3 cases. Metal content in the plate increases as power index increases. This leads to decrease in buckling temperature.

Figures 8 and 9 show the variation of critical buckling temperature for FGM plate under non-uniform temperature distribution across thickness. Qualitatively the results obtained for both uniform (Figs.6-7) and non-uniform (Figs.8-9) temperature distribution cases are the same. However, results obtained with non-uniform temperature distribution (Figs. 8-9) predicts substantially more critical buckling temperature as compared to uniform temperature distribution case (Figs. 6-7). Figs.10-11 show the effect of temperature dependent material properties on critical buckling temperature for uniform temperature case. Here one could note that temperature dependent material properties causes substantial (around 25 per cent) decrease in critical buckling temperature of the FGM plate for BC1, BC2 and BC3 cases. This is because of the fact that increase of temperature causes reduction in stiffness of the plate. These results obtained for FGM plate with cutout

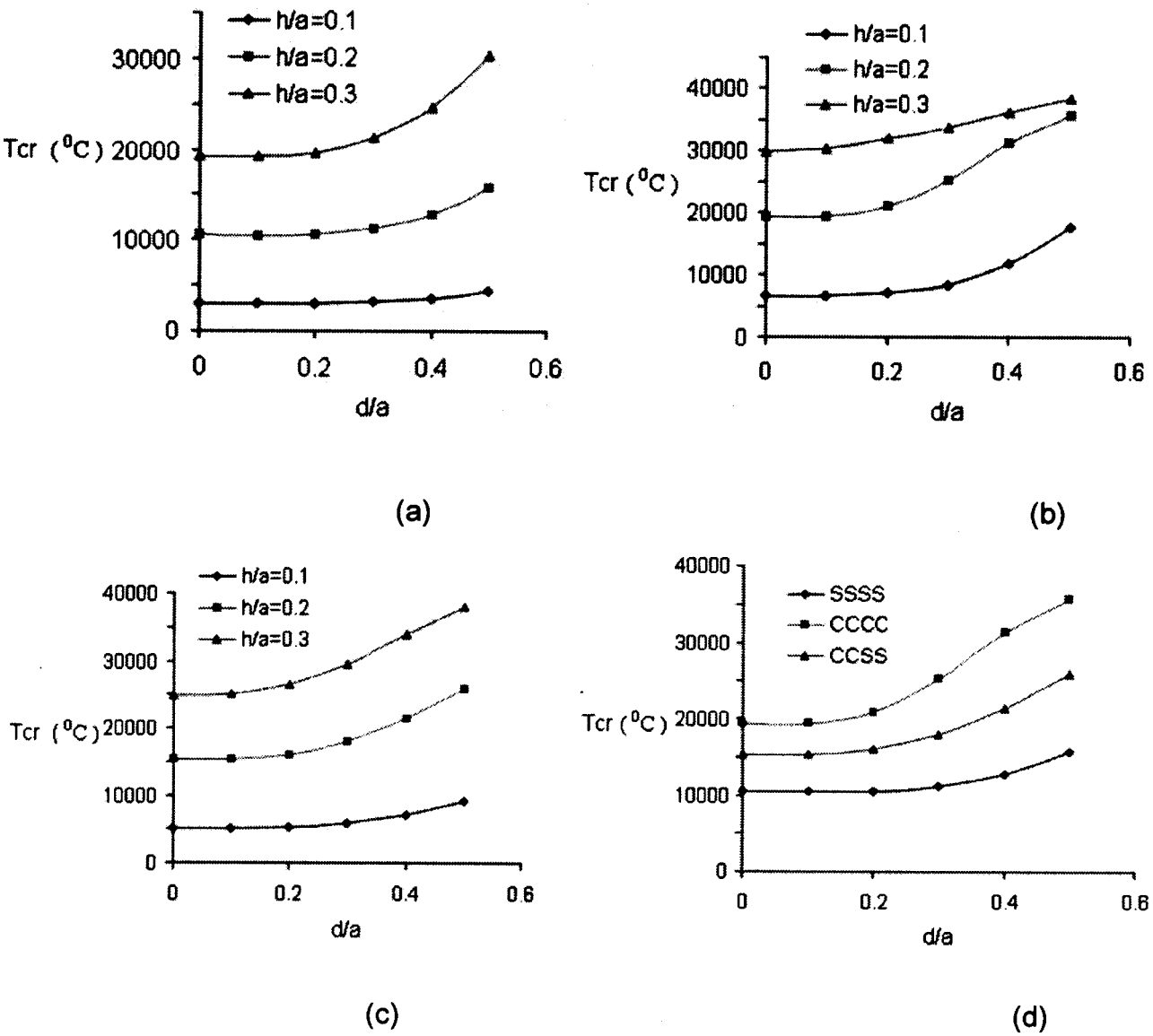

Fig.8 Critical buckling temperature vs the sizes of the cutout in the FGM plate under non-uniform temperature, (a/b=1, k=1) for (a) BC1 (b) BC2, (c) BC3 boundary conditions and (d) BC1, BC2 and BC3 boundary conditions (h/a=0.2)

are similar to the thermal buckling results of isotropic and composite plates with cutout by Chang and Shiao [21]. Figs.12-13 shows the effect of temperature dependent material properties on critical buckling temperature for non-uniform temperature case. Here also temperature dependent material properties causes substantial (around 25 per cent) decrease in critical buckling temperature of the FGM plate for BC1, BC2 and BC3 cases. These results obtained for FGM plate with cutout are similar to corresponding results of Chang and Shiao [21] for composite plates with cutout.

Conclusions

Based on first order shear deformation theory finite element code is developed. The developed computer code is validated for thermal buckling of isotropic and FGM plates. Results obtained from present finite element analysis do agree with those reported in the literature. Critical

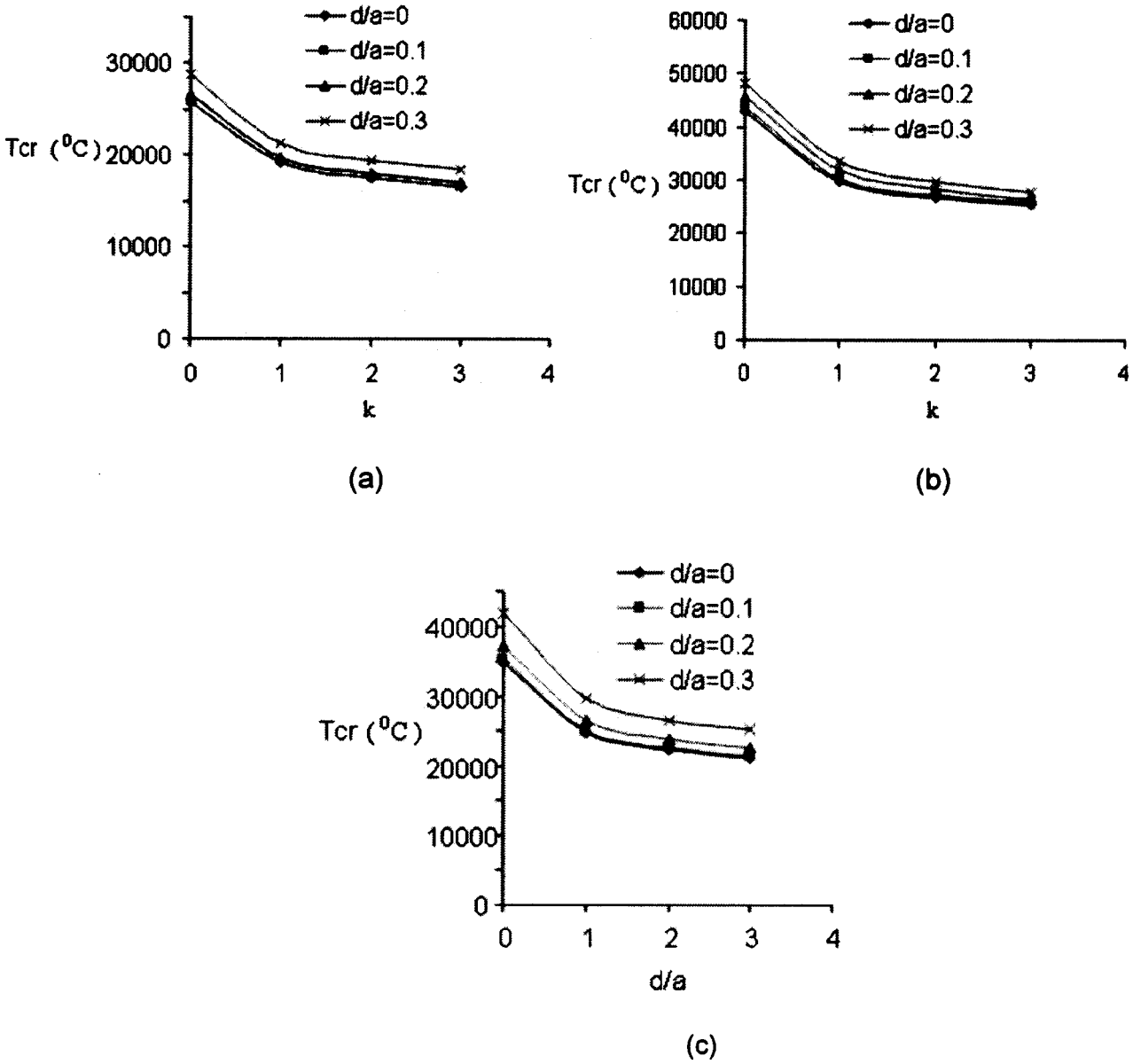

Fig.9 Critical buckling temperature vs power index 'k' of the FGM plate under non-uniform temperature, (a/b=1, h/a=0.3) (a) BC1 (b) BC2 and (c) BC3 boundary conditions

buckling loads of square FGM plate with circular cutout are computed. Uniform and non uniform temperature distributions across the FGM plate thickness are considered. Further, FGM material properties are considered to be temperature dependent. Effects of (i) plate aspect ratio, (ii) plate thickness to side ratio, (iii) power index '*k*' and (iv) size of the cutout and (v) the three different boundary conditions on the critical buckling temperature are investigated. Based on the present numerical results following conclusions are made.

- Critical buckling temperature increases with increase in radius of the cutout in the rectangular FGM plate.
- Critical buckling temperature of the FGM plates increases with increase in thickness to span ratio.
- Critical buckling temperatures of the FGM plates decrease with increase in power law index '*k*'.
- Critical buckling temperatures of the FGM plates are decreased when material properties are considered to be function of temperature as compared to the results obtained where material properties are assumed to be independent of temperature.
- Critical buckling temperatures for BC1 (SSSS) boundary condition are larger than the corresponding temperatures obtained for BC2 (CCCC) and BC3 (CCSS) boundary conditions.

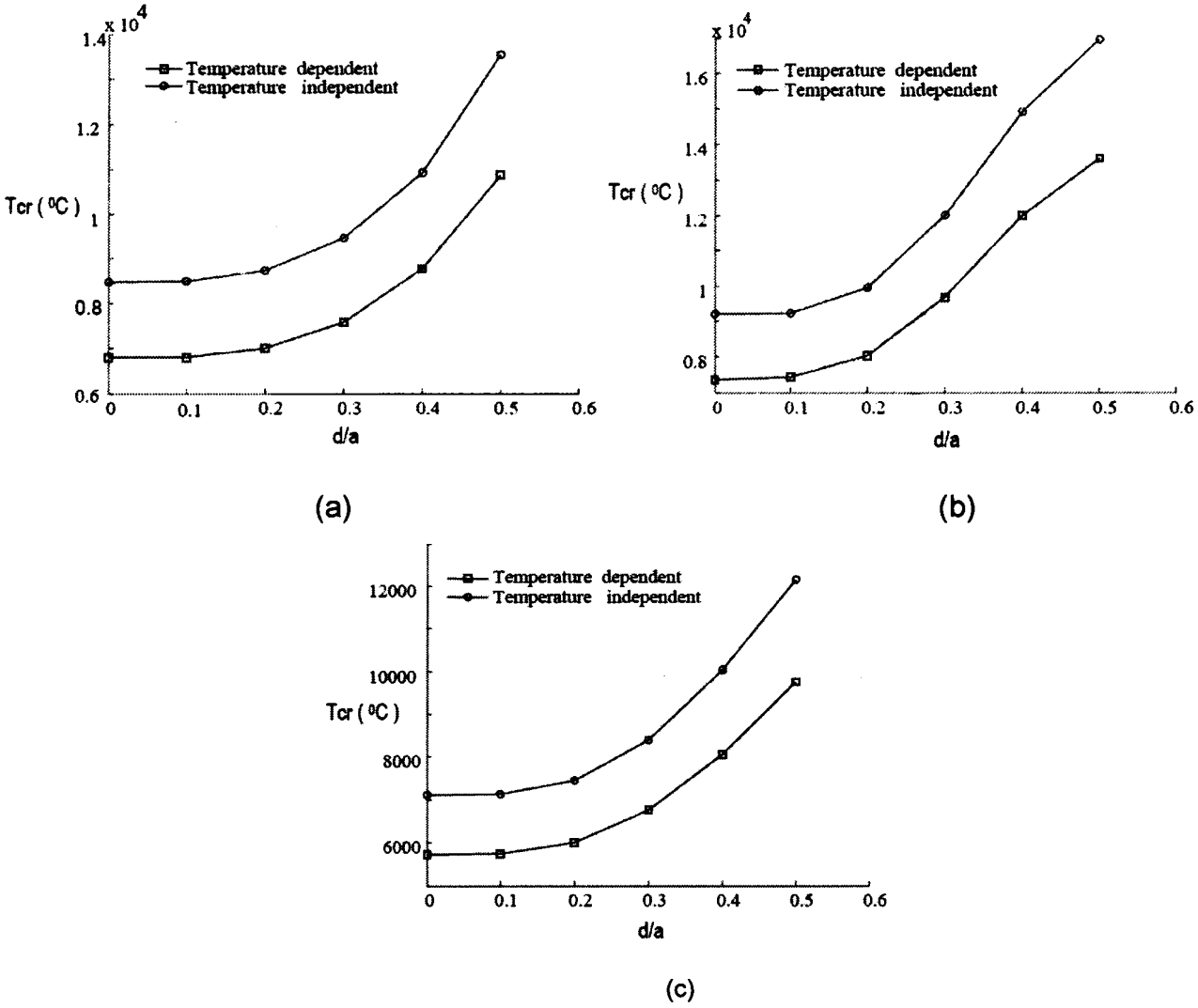

Fig.10 Effect of temperature dependent material properties and cutout size on critical buckling temperature of the FGM plate under uniform temperature,(a/b=1, k=1, h/a=0.3) for (a) BC1 (b) BC2 and (c) BC3 boundary conditions

Acknowledgement

Author gratefully acknowledge the research grant of AR & DB, Structures Panel DARO/08/105321/2005 SRIC/ABJ.

References

1. Ravichandran, K.S.,"Thermal Residual Stresses in a Functionally Graded Material System", Journal of Materials Science and Engineering, Vol.A201, pp. 269-276, 1995.

2. Praveen, G.N. and Reddy, J. N.,"Nonlinear Transient Thermoelastic Analysis of Functionally Graded Ceramic Metal Plates". International Journal of Solids and Structures,Vol.35, pp. 4457-4476, 1998.

3. Pradhan, S.C., Loy, C.T., Lam, K.Y. and Reddy J.N., "Vibration Characteristics of Functionally Graded Cylindrical Shells under Various Boundary Conditions", Journal of Applied Acoustics, Vol.6, No.1, pp.111-129, 2000.

4. Cho, J.R. and Oden, J.T., "Functionally Graded Material - A Parametric Study on Thermalstress Characteristics using the Crank-Nicolson-Galerkin Scheme", Journal of Computer Methods in Applied Mechanics and Engineering, Vol.188, pp.17-38, 2000.

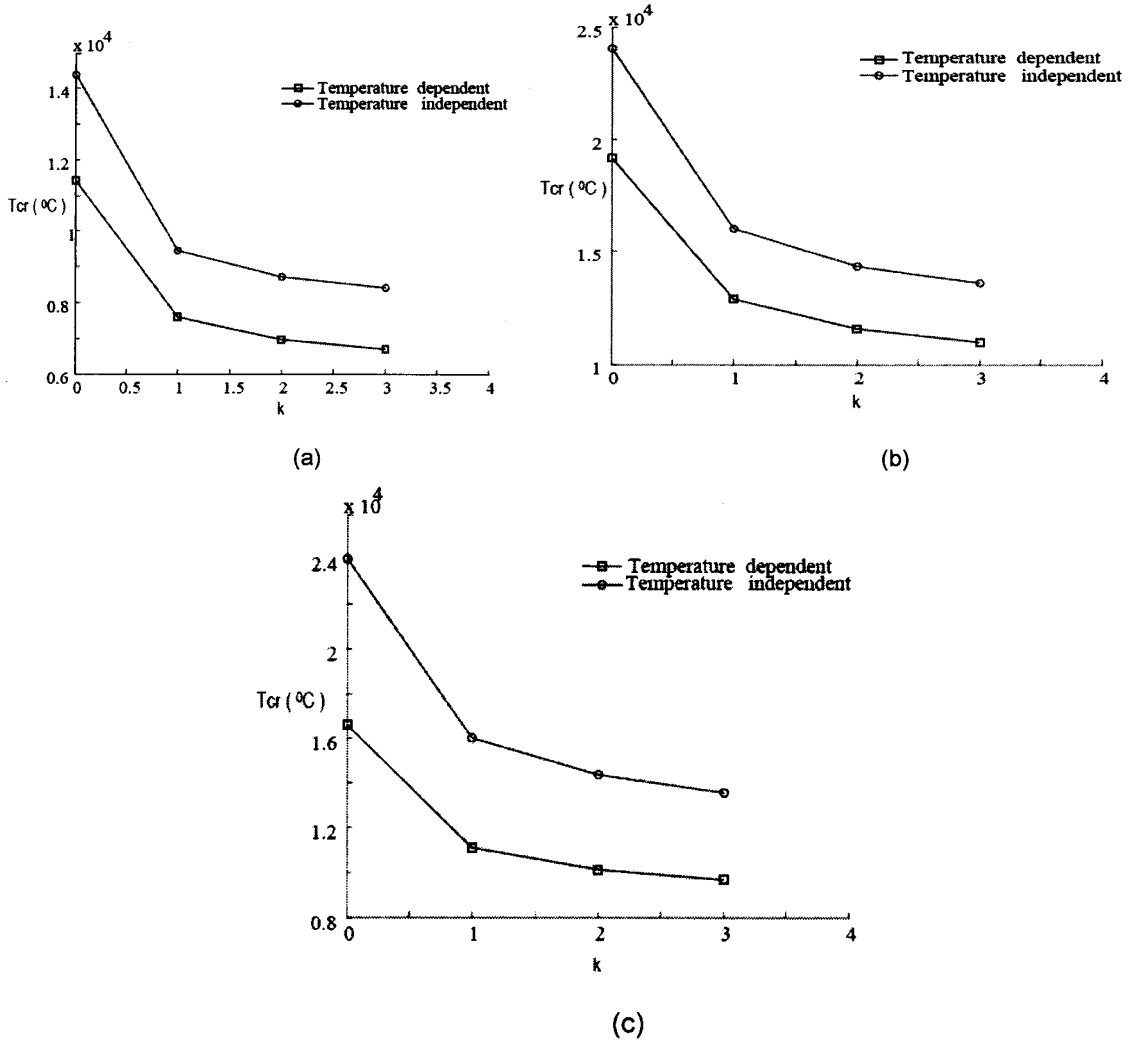

Fig.11 Effect of temperature dependent material properties and power index 'k' on critical buckling temperature of the FGM plate under uniform temperature,(a/b=1, d/a=0.3, h/a=0.3) for (a) BC1 (b) BC2 and (c) BC3 boundary conditions

5. Reddy, J.N., "Analysis of Functionally Graded Plates", International Journal for Numerical Methods in Engineering, Vol. 47, pp. 663-684, 2000.

6. Woo, J. and Meguid, S.A., "Nonlinear Analysis of Functionally Graded Plates and Shallow Shells", International Journal of Solids and Structures, Vol.38, pp.7409-7421, 2001.

7. Kim, K.S. and Noda, N., "A Green's Function Approach to the Deflection of a FGM Plate under Transient Thermal Loading", Journal of Archive of Applied Mechanics, Vol.72, pp.127-137, 2002.

8. Tsukamoto, H., "Analytical Method of Inelastic Thermal Stresses in a Functionally Graded Material plate by a Combination of Micro and Micromechanics", Journal of Composites, 2003, Vol.34, Part-B, pp. 561-568, 2003.

9. Yang, J., Kitipornchai, S. and Liew, K.M., "Large Amplitude Vibration of Thermo-electromechanically Stressed FGM Laminated Plates", Journal of

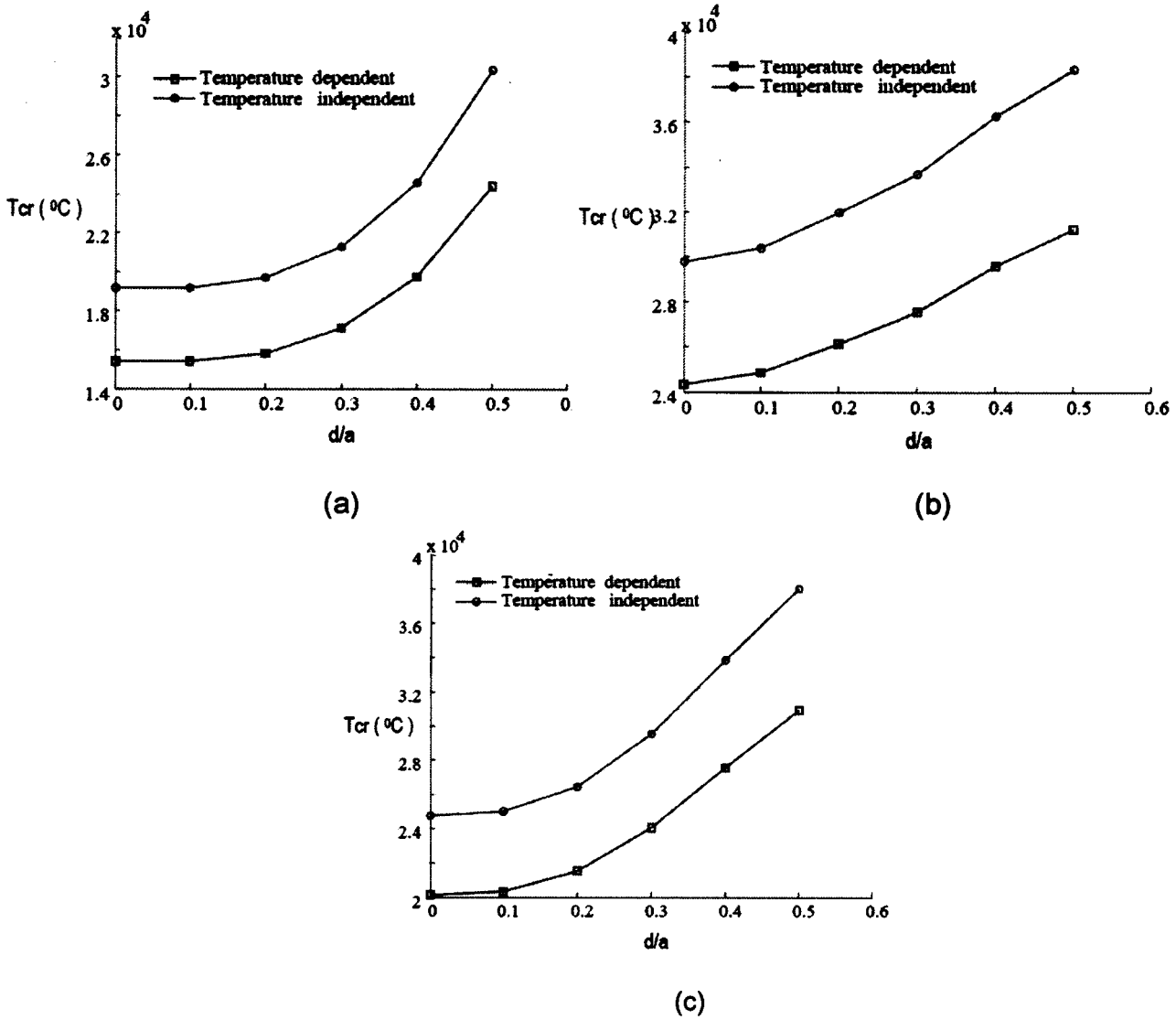

Fig.12 Effect of temperature dependent material properties and cutout size on critical buckling temperature of the FGM plate under non-uniform temperature,(a/b=1, k=1, h/a=0.3) for (a) BC1 (b) BC2 and (c) BC3 boundary conditions

Computer Methods in Applied Mechanics and Engineering, Vol.192, pp.3861-3885, 2003.

10. Ma, L.S. and Wang, T.J.,"Nonlinear Bending and Post-buckling of a Functionally Graded Circular Plate under Mechanical and Thermal Loadings", International Journal of Solids and Structures, Vol. 40, pp.3311-3330, 2003.

11. Croce, L.D. and Venini, P., "Finite Elements for Functionally Graded Reissner-Mindlin Plates", Journal of Computer Methods in Applied Mechanics and Engineering, Vol.193, pp.705-725, 2004.

12. Najafizadeh, M.M. and Heydari, H.R., "Thermal Buckling of Functionally Graded Circular Plates Based on Higher Order Shear Deformation Plate Theory", European Journal of Mechanics A/Solids, Vol. 23, pp.1085-1100, 2004.

13. Lanhe, W., "Thermal Buckling of a Simply Supported Moderately Thick Rectangular FGM Plate", Composite Structures, Vol. 64, pp.211-218, 2004.

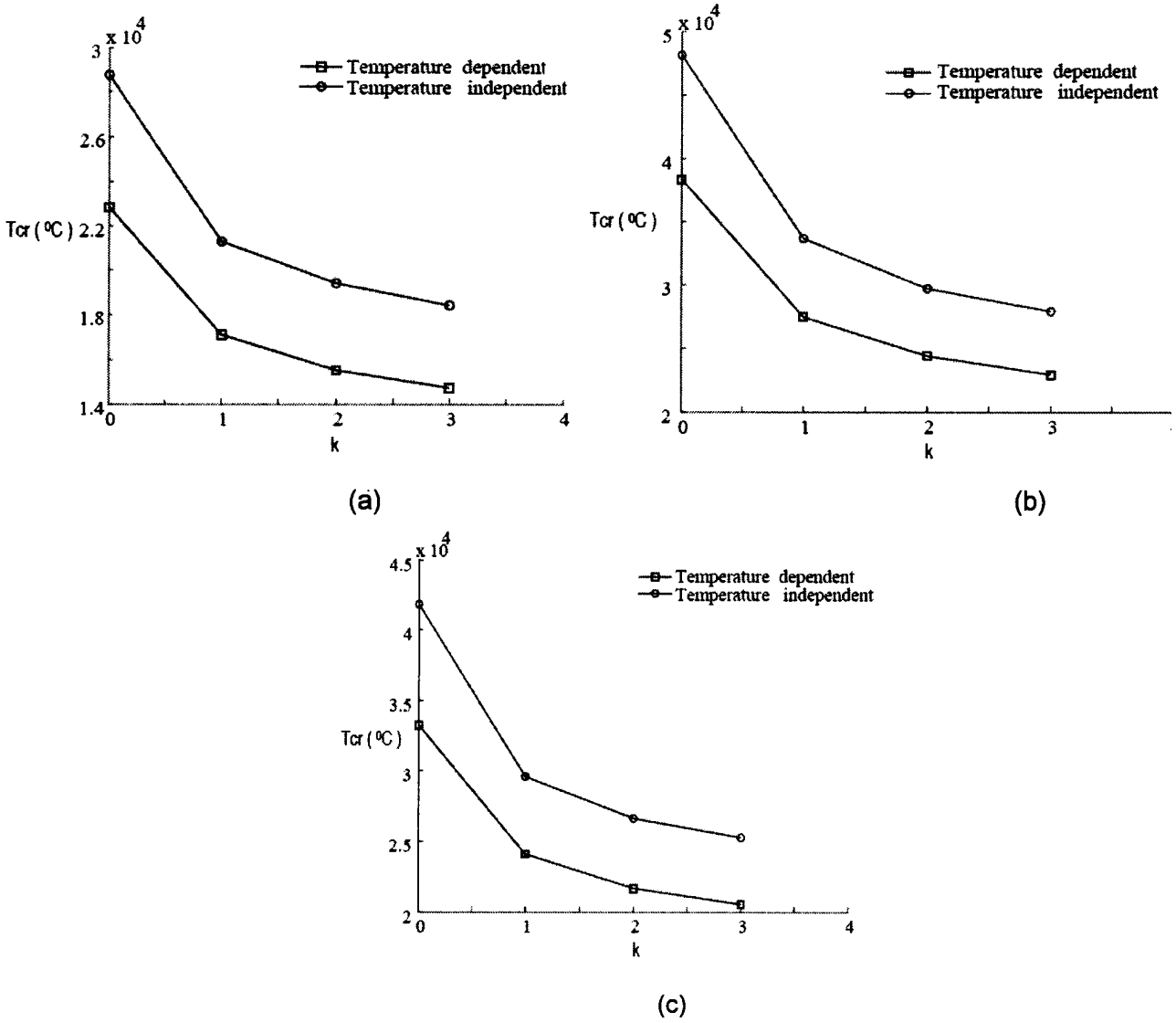

Fig.13 Effect of temperature dependent material properties and power index 'k' on critical buckling temperature of the FGM plate under non-uniform temperature,(a/b=1, d/a=0.3, h/a=0.3) for (a) BC1 (b) BC2 and (c) BC3 boundary conditions

14. Pradhan, S.C., "Vibration Suppression of FGM Composite Shells using Embedded Magnetostrictive Layers", International Journal of Solids and Structures, Vol. 42, No. 9-10, pp.2465-2488, 2005.

15. Shen, H.S., "Post-buckling of FGM Plates with Piezoelectric Actuators under Thermoelectro-mechanical Loadings", International Journal of Solids and Structure, Vol. 42, No.23, pp. 6101-6121, 2005.

16. Sladeka, J., Sladeka, V. and Zhangb, Ch.,"Stress Analysis in Anisotropic Functionally Graded Materials by the MLPG Method", Journal of Engineering Analysis with Boundary Elements, Vol. 29, pp.597-609, 2005.

17. Yang, J., Liew, K.M. and Kitipornchai, S., "Second-order Statistics of the Elastic Buckling of Functionally Graded Rectangular Plates", Journal of Composites Science and Technology, Vol.65, pp.1165-1175, 2005.

18. Dai, K.Y., Liu, G.R., Han, X. and Lim, K.M., "Thermo-mechanical Analysis of Functionally Graded Material (FGM) Plates using Element-free Galerkin Method", Computers and Structures, Vol.83, pp.1487-1502, 2005.

19. Kyung, S.N. and Kim, J.H., "Three-dimensional Thermo-mechanical Buckling Analysis for Functionally Graded Composite Plates", Composite Structures, Vol.73, No.4, pp.413-422, 2006.

20. Huang, X.L. and Shen, H.S.,"Vibration and Dynamic Response of Functionally Graded Plates with Piezoelectric Actuators in Thermal Environments", Journal of Sound and Vibration, Vol.289 (1,2,3), pp.25-53.

21. Chang, J.S. and Shiao, F.J., "Thermal Buckling Analysis of Isotropic and Composite Plates with a Hole", Journal of Thermal Stresses, Vol.13, pp.315-332, 1990.

22. Chen, W.J., "Thermal Buckling Behavior of Thick Composite Laminated Plates under Non-uniform Temperature Distribution", Computers and Structures, Vol.41, pp.637-645, 1991.

23. Prabhu, M.R. and Dhanaraj, R., "Thermal Buckling of Laminated Composite Plates", Computers and Structures,Vol. 53, No.5, pp.1193-1204, 1994.

24. Shen, H.S. and Noda, N., "Postbuckling of FGM Cylindrical Shells under Combined Axial and Radial Mechanical Loads in Thermal Environments", International Journal of Solids and Structures, Vol.42, pp.4641-4662, 2005.

25. Boley, B.A. and Weiner, J.H. "Theory of Thermal Stresses", John Wiley, 1960.